Robust Adaptive Control of a Large Spacecraft

Shinichi Tsuda and Koichi Sakano

Abstract--**This paper deals with the applicability of Robust Adaptive Control to the attitude motion control of large spacecraft. Large spacecraft and space structures, such as large communication satellites and the ISS (International Space Station), have been constructed on orbit. However dynamic characteristics of these structures can not be fully verified on the ground because of their size, mass and flexibility. Therefore, some unmodelled dynamics, for example, truncated vibration modes, and/or unknown elements should be taken into account for the precise and stable control of attitude motion. Based on the above consideration the applicability of the Robust Adaptive Control was carefully examined and the results of numerical simulations are given. These showed good performance of the attitude control system. We also refer to the basic idea about the modal truncation.**

Key words—**Adaptive Control, Flexible Structure, Robust Control, Satellite**

I. Introduction

In recent years large spacecrafts and space structures have been constructed on orbit. In general, dynamic characteristics of these structures are not able to be fully verified by testing on the ground. Basically such space structures have infinite number of vibration modes because of its nature of distributed parameter system. Mathematical modeling by the Finite Element Method (FEM) is used for the control system design and analysis, however, this model usually contains the errors, especially in higher order modes. Some additional considerations must be taken into account with compared to classical control synthesis. To some extent, truncation of the modes is inevitable to model the dynamics of the structure. The truncation error should be considered for the control system design to avoid the so-called spill-over phenomena. In order to realize this, the robust control design approach, such as H-infinity controller, has been studied. Although the results have been obtained, such as in reference [1], it is troublesome to establish weighting functions in the frequency domain to characterize the higher order dynamics of the vibration modes, that is, unmodeled dynamics by the truncation. This also includes trial and error operations to optimize the control performance.

Based on the above considerations the authors propose an application of the Robust Adaptive Control, which has not been tried yet for the spacecraft attitude control. In the control synthesis it is not required to define those weighting function, instead, a few parameters, which is not directly related to unmodeled dynamics, have to be incorporated in the control algorithm. This is much simpler and easier than the H-infinity optimization process.

In this paper, based on the usual MRACS (Model Reference Adaptive Control System), robust adaptive control law is synthesized. The ε-modification method was adopted among some methods. The effectiveness of this approach was verified by numerical simulations using a spacecraft model described below.

Fig.1 shows a typical large spacecraft, Japanese Engineering Test Satellite VI (ETS-VI), which was launched from Tanegashima Space Center in 1994 for advanced satellite communication experiments. It weighs about 2000kg at the initial orbit and the span of both solar arrays is almost 30m. Several antennas were deployed on orbit and the largest one is 5m in diameter. These are flexible appendages attached to the center body of the spacecraft. We will discuss an applicability of the Robust Adaptive Control using this ETS-VI model.

II. Mathematical Model of ETS-VI

A mathematical model of the spacecraft including flexible appendages is expressed in the following modal equations:

$$\ddot{\eta}_i + 2\zeta_i\omega_i\dot{\eta}_i + \omega_i^2\eta_i = \phi_i u_P \tag{1}$$

$$\theta = \sum_i \phi_i\eta_i \tag{2}$$

where η_i, ω_i and ζ_i are the i-th modal coordinate, the i-th modal frequency and the i-th modal damping, respectively. ϕ_i is the i-th mode shape and θ is an attitude angle of the spacecraft. Control torque is given by u_p. And these variables have appropriate dimensions.

From the above equations we obtain the transfer function from u_p to θ (hereinafter, replaced by y_p) as follows.

$$\frac{y_P}{u_P} = \sum_i \frac{\phi_i^2}{s^2 + 2\zeta_i\omega_i s + \omega_i^2} \tag{3}$$

In this study we take the first and second modes, i.e., $i = 1, 2$, into account as a known model and two higher modes will be incorporated as unmodeled dynamics. These modes are

Manuscript received July 24, 2008.

S. Tsuda is with the Department of Aeronautics and Astronautics, School of Engineering, Tokai University, Hiratsuka, Japan. (e-mail::stsuda@keyaki.cc.u-tokai.ac.jp)

K. Sakano is with Mitubishi Electric Engineering, Kamakura, Japan (e-mail.:amx-002@ezweb.ne.jp)

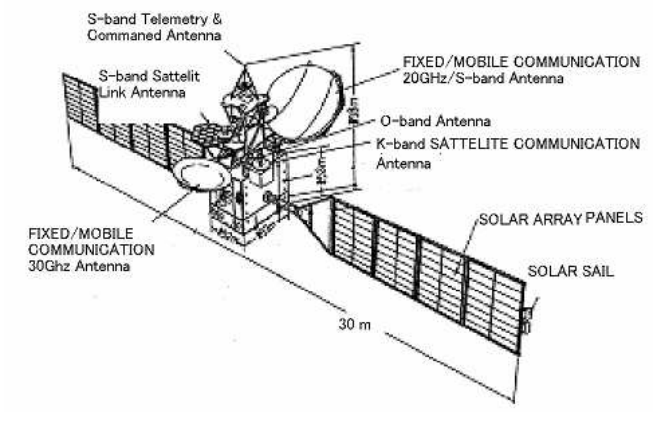

Fig.1 Configuration of ETS-Ⅵ

considered to be truncated modes in which modeling errors might be larger than the lower modes as pointed before.

Further higher modes are completely neglected in this study. We also briefly refer to a rationale about this truncation of the higher modes as follows. Basically the contribution of the higher modes to the spacecraft attitude motion, i.e., torque generated by these mode vibration, becomes smaller with compared to the lower modes. If this is not true, then, the usual truncation does not make sense. We can further state that the damping of the higher modes is usually much larger than that of the lower modes. This is because the modal shapes of higher modes are much complicated. Especially, the structure of late years is made of composite materials and then, the matrix and the adhesive make the damping much larger. And at the same time the oscillation of higher modes decays rapidly in a short time. These ideas are summarized in Fig.2.

In this chart frequency range is divided into three categories, low, high and higher. Low frequency modes are usually incorporated in the control design. Also a portion of high frequency modes and higher modes will be truncated.. As noted above, higher frequency modes essentially have large damping and rapid decay, therefore, their effect dissipates very quickly. Based on our experience usually 5 or 6 modes were verified by FEM analysis and by ground testing like modal survey. Nevertheless modal parameters of the high frequency modes will be not accurate, and this is 'the state of the art'.

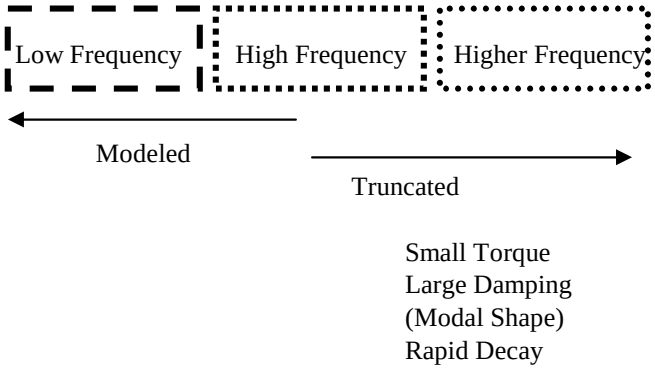

Fig.2 Mode Classification

III. Robust Adaptive Control Law

The 'Actual Plant' is modeled as follows.

$$y_p = (G_p(s) + \Delta_a(s)) \cdot u_p \tag{4}$$

where $G_p(s)$ is given below and represents the known model portion of the plant.

$$G_p(s) = k_p \frac{Z_p(s)}{R_p(s)} \tag{5}$$

$Z_p(s), R_p(s)$ are monic polynomials with the order of m_p, n_p, respectively. And k_p is a constant, which is called high frequency gain. $\Delta_a(s)$ is additive, unmodeled dynamics of the plant.

The reference model is defined as below:

$$y_m = W_m(s) \cdot r = k_m \frac{Z_m(s)}{R_m(s)} \cdot r \tag{6}$$

where r is the reference input. Eqs. (4)- (6) are assumed to satisfy the following conditions[2],[3].

1) $\Delta_a(s)$ is strictly proper transfer function,

2) high frequency gain k_p in $G_p(s)$ is known,

3) the relative order of $G_p(s)$, $n^* = n_p - m_p$, is known and the relative order of $W_m(s)$ is equal to that of $G_p(s)$, and

4) $G_p(s)$ and $W_m(s)$ are minimum phase system.

The above assumptions are the same as in the usual MRACS and an adaptation mechanism makes the plant output follow that of the reference model.

Fig.3 shows the block diagram of the adaptive control system which includes the unmodeled dynamics in the unknown plant.

The adaptive controller is illustrated in Fig.4.

The additive unmodeled dynamics is represented by a block diagram as shown in Fig.5.

The adaptive control law is given by

$$u_p = \theta_0^T(t)\omega_0 + c_0^* r + u_a \tag{7}$$

where

$$\theta_0 = [\theta_1^T, \theta_2^T, \theta_3]^T,$$

$$\omega_0 = [\omega_1^T, \omega_2^T, y_p]^T, c_0^* = \frac{k_m}{k_p}, \omega_1 = \frac{\alpha(s)}{\Lambda(s)} u_p,$$

$$\omega_2 = \frac{\alpha(s)}{\Lambda(s)} y_p, \alpha(s) = [s^{n_p-2}, \cdots, s, 1]^T,$$

and $\Lambda(s) = \Lambda_0(s) Z_m(s)$ is the $(n_p - 1)$ th order stable polynomial.

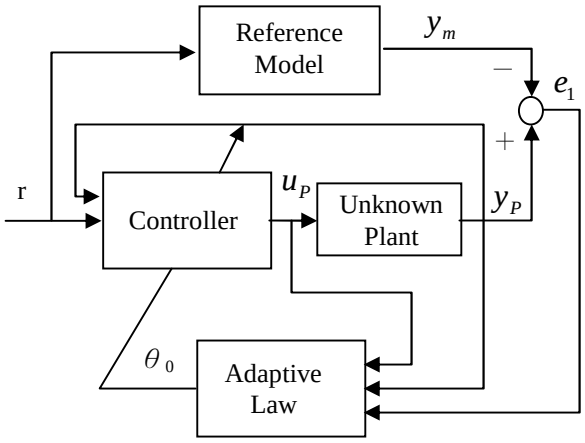

Fig.3 Block Diagram for Robust MRACS

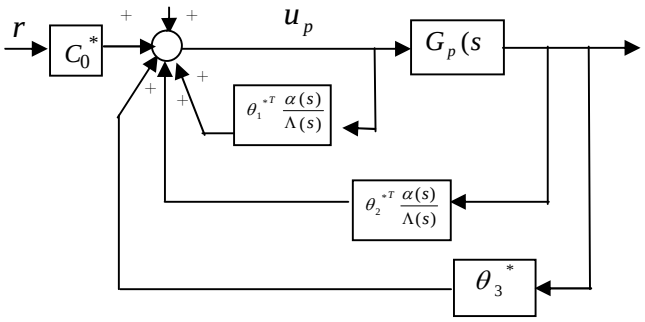

Fig.4 Robust Adaptive Controller

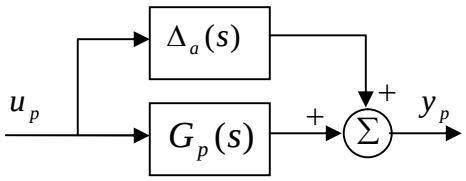

Fig.5 Representation of Unknown Plant

A robust adaptive law is shown below. For the generation of parameter vector θ_0, the $\varepsilon-$modification was adopted.

$$\dot{\theta}_0 = \Gamma\varepsilon\phi_0 - \Gamma\omega\theta$$
$$\omega = |\varepsilon m|\nu_0$$
$$\varepsilon = \frac{z-\theta_0^T\phi_0}{m^2}$$
$$m^2 = 1+n_s^2, \quad n_s^2 = m_s$$
$$\dot{m}_s = -\delta_0 m_s + u_p^2 + y_p^2, \quad m_s(0) = 0$$
$$\phi_0 = W_m(s)\omega_0$$

where $z = W_m(s)u_p - c_0^* y_p$ *and* $\Gamma = \Gamma^{-1} > 0$ are adaptive gains, and $\nu_0 > 0$ *and* $\delta_0 > 0$ are design parameters.

These have to be specified in the controller design procedure and some tuning would be required in order to optimize the controller performance.

The auxiliary input u_a is given by the following.

$$u_a = -C(s)e_1$$
$$e_1 = \frac{1}{c_0^*}W_m(s)[\tilde{\theta}_0^T\omega_0 + u_a + d_1]$$
$$d_1 = \frac{\Lambda(s)-\theta_1^{*T}\alpha(s)}{\Lambda(s)}G_p^{-1}(s)\Delta_a(s)$$
$$C(s) = \frac{c_0^* W_m^{-1}(s)}{(\tau s+1)^{n^*}-1}$$

where $\tau > 0$ is a design parameter. $C(s)$ is called a model error compensator and specified to make the auxiliary input u_a smaller as the tracking error e_1 becomes smaller. The above adaptive law assures the robust stability in the case that the plant has unknown element.

IV. Controller Design

A known plant is represented as follows.

$$G_p(s) = \frac{\phi_1^2}{s^2} + \frac{\phi_2^2}{s^2+2\zeta_2\omega_2 s+\omega_2^2}$$

In this study $n_p = 4, m_p = 2$ *and* $n^* = 2$ are assumed for the design of adaptive control law. The 3 rd and 4 th vibration modes are assumed unmodeled dynamics. In the ETS-VI model the 1 st mode is a rigid body mode, and 2 nd, 3 rd and 4 th modes are out-of-plane vibration modes of solar array panels.

Then additive unmodeled dynamics is given by the following summation of 3 rd and 4 th modes.

$$\Delta_a(s) = \frac{\phi_3^2}{s^2+2\zeta_3\omega_3 s+\omega_3^2} + \frac{\phi_4^2}{s^2+2\zeta_4\omega_4 s+\omega_4^2}$$

Modal parameters used here are shown in Table 1. Also modal shapes are illustrated in Fig.6

Table 1. Modal Parameters[1]

	Rigid Body	1 st OoP*	2 nd OoP	3 rd OoP
frequency [Hz]	0	0.196	0.834	2.196
Damping	—	0.005	0.005	0.005

*OoP: Out of Plane

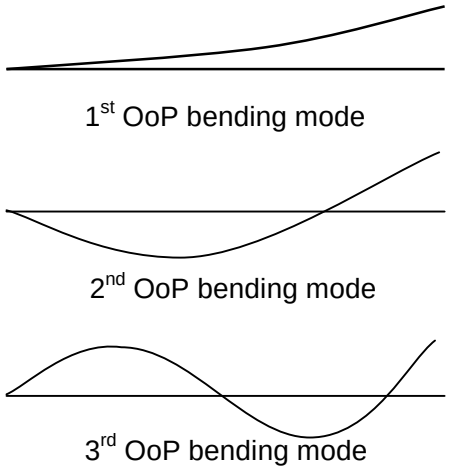

Fig.6 Modal Shapes of Solar Array

The transfer function given below is a reference model for our simulation study.

$$y_m = \frac{1}{7200}\left(\frac{1}{s^2} + \frac{1}{s^2 + 1.414s + 1}\right) \cdot r$$

This consists of rigid body dynamics and the second order system which has a large damping ratio with compared to the actual plant.

The design parameters in the control and adaptive laws are assumed to be the following numbers.

$$\Lambda(s) = s^3 + 1.207s^2 + 0.8535s + 0.25$$

$$\Gamma = 5, \nu_0 = 0.5, \delta_0 = 0.0004$$

$$\tau = 0.4$$

It is noted again that the design parameters selection is arbitrary under a few constraints, therefore, some design effort might be necessary to obtain the satisfactory performance.

V. Simulation Results

In this section numerical simulation results will be shown to verify the applicability of the robust adaptive control.

As a reference input, pulse doublet, given by Fig.7, was used for simulations. This doublet torque is for the attitude control from rest to rest .

Fig.8 shows the attitude motion of the spacecraft without control. An oscillation with slightly damping is maintained.

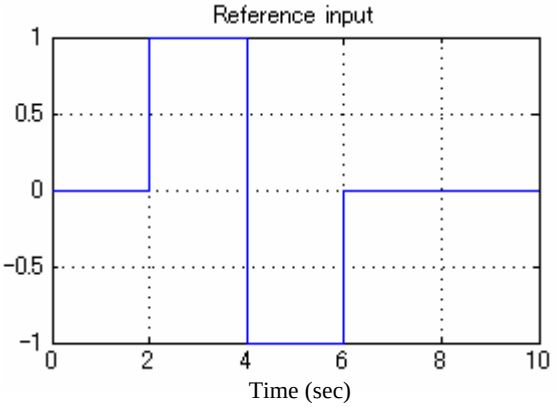

Fig.7 Reference input [Nm]

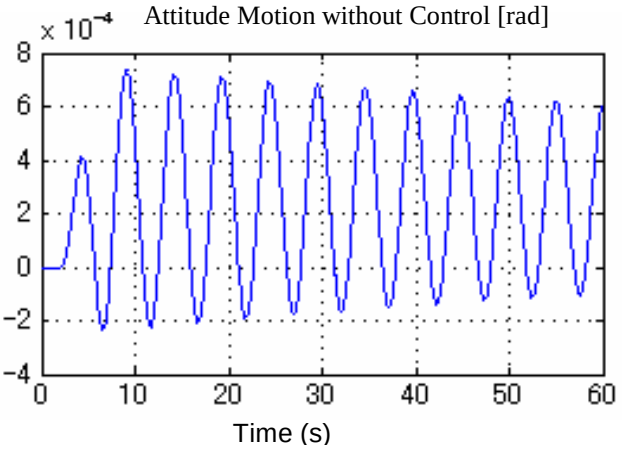

Fig.8 Attitude Motion without Control

By incorporating the robust adaptive control, output of the reference model, the actual plant and tracking error are illustrated in Figs. 9～11. From the tracking error it is found that the output of actual plant follows the reference model output. Tracking error shortly converges and oscillatory motion is not observed. Truncated higher mode effects are suppressed in the output.

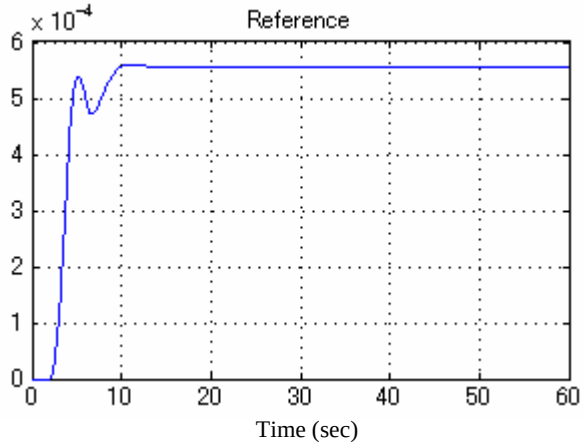

Fig.9 Output of Reference Model [rad]

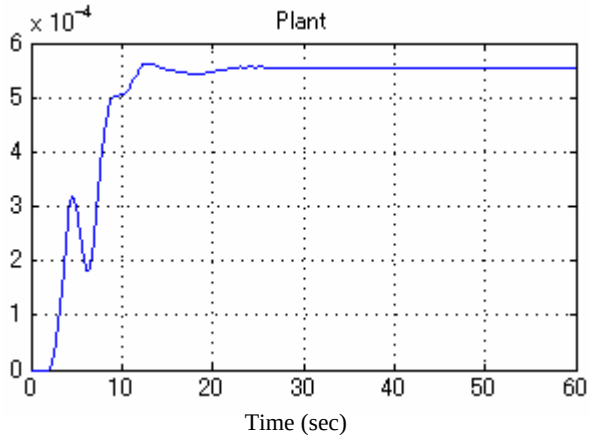

Fig.10 Output of Actual Plant [rad]

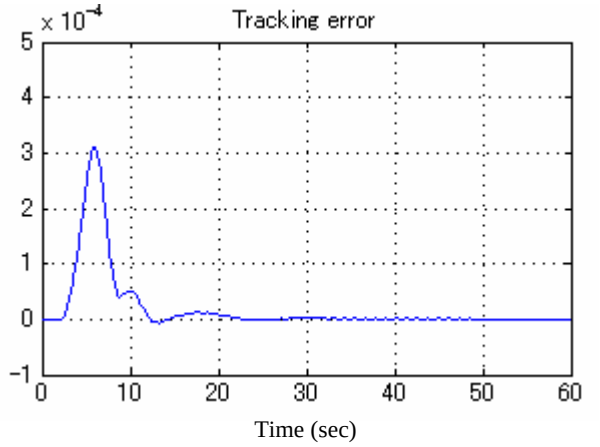

Fig.11 Output of Tracking Error [rad]

VI. Conclusion

Large spacecrafts have the flexibility with infinite number of vibration modes which must be taken into account in the control system design. And their damping ratio is so small that oscillatory motion has to be damped by an appropriate control method. Furthermore it is very difficult to precisely get the modal parameters, especially for higher modes, by ground testing and mainly we depend on modal analysis by FEM. However the error of modal parameters, modal frequency and modal damping, is inevitable.

The robust adaptive control system was formulated and applied to the large spacecraft attitude motion control. By the numerical simulations the validity of this approach has been demonstrated. Some efforts might be required to specify parameters for the control algorithm.

Although few applications have been reported so far, our approach would be one of the solutions to deal with unknown structural flexibility of spacecraft and large space structure.

References

[1] K. Yamaguchi, et al,: 'On orbit ETS-VI attitude control experiments by robust control' NAL report, No. 1348,1998 (in Japanese)

[2]J. Sun: 'Modified Reference Adaptive Control Scheme for Improved Transient Performance' Proceeding of 1991 American Control Conference, pp150-155, 1991.

[3]P. A. Ioannou and J. Sun: 'Theory and design of robust direct and indirect adaptive control schemes', Int. Journal of Control, Vol.47, no.3, pp.775-813, 1988.

[4]P. A.Ioannou and J. Sun: 'ROBUST ADAPTIVE CONTROL' Prentice Hall, 1996